Supplementary Materials

Simple Fluorene Oxadiazole-based Ir(III) Complexes with AIPE Property: Synthesis, Explosive Detection and Electroluminescence Studies

Jia-Wei Liu,[a] Ya-Nan Xu,[a] Chun-Yan Qin,[a] Zi-Ning Wang,[a] Cong-Jin Wu,[a] Yong-Hua Li,*[a] Shi Wang,*[a] Kenneth Yin Zhang*[a] and Wei Huang*[ab]

[a] *Key Laboratory for Organic Electronics and Information Displays & Institute of Advanced Materials (IAM), Jiangsu National Synergistic Innovation Center for Advanced Materials (SICAM), Nanjing University of Posts & Telecommunications, Nanjing 210023, China.*

E-mail: iamswang@njupt.edu.cn; *iamyzhang@njupt.edu.cn*; *iamyhli@njupt.edu.cn*; *iamwhuang@nwpu.edu.cn*
http://smse.njupt.edu.cn/

[b] *Institute of Flexible Electronics, Northwestern Polytechnical University, Xi'an 710000, China.*

Table of Contents

Synthesis of 2-bromo-9,9-dihexyl-9H-fluorene (2)

A mixture of 2-bromo-9H-fluorene **1** (5 g, 20 mmol), TBAB (0.3287 g, 1.025 mmol), 50% NaOH 2 mL, DMSO 20 mL was stirred 12 h at 50 ^{o}C. After cooling to room temperature, the solution was poured into water and extracted with dichloromethane. The organic phase was dried over anhydrous sodium sulfate, filtered, and concentrated to dryness. The crude was purified by column chromatography on silica gel to afford a transparent liquid **2** (7.525 g, 18.22 mmol, 89%). ^{1}H NMR (400 MHz, $CDCl_3$) δ = 7.70 (s, 1H), 7.59 (d, *J*=7.8, 1H), 7.56 – 7.45 (m, 2H), 7.36 (s, 3H), 2.00 (d, *J*=4.1, 4H), 1.14 (dd, *J*=18.4, 11.5, 12H), 0.82 (t, *J*=6.2, 6H), 0.74 (s, 4H).^{13}C NMR (101 MHz, $CDCl_3$) δ 151.43, 145.75, 139.18, 131.30, 129.01, 127.30, 126.48, 123.12, 120.87, 120.26, 119.88, 109.95, 77.54, 77.22, 76.90, 55.51, 40.14, 31.48, 29.60, 23.72, 22.57, 14.03.

Synthesis of 2-cyano-9,9-dihexyl-9H-fluorene (3)

A mixture of compound **2** (7.525 g, 18.22 mmol), CuCN (3.275 g, 28.95 mmol) was dissolved in dry and degassed DMF 25 mL, and stirred for 24 h at 155 ^{o}C under a nitrogen atmosphere. After cooling to room temperature, ammonia was added to the solution to dissolve CuCN and precipitated product. After stirring for 30 min, the mixed solution was filtered and washed with water. The crude was purified by column chromatography on silica gel to afford a pale yellow liquid **3** (5.225 g, 14.47 mmol, 80%). ^{1}H NMR (400 MHz, $CDCl_3$) δ = 7.75 (td, *J*=6.0, 1.4, 2H), 7.66 – 7.60 (m, 2H), 7.43 – 7.33 (m, 3H), 2.00 (dd, *J*=10.6, 6.1, 4H), 1.21 – 0.95 (m, 12H), 0.76 (t, *J*=7.1, 6H), 0.66 – 0.50 (m, 4H).^{13}C NMR (101 MHz, $CDCl_3$) δ 151.43 (d, J = 7.4 Hz), 145.75, 139.18, 131.30, 129.01, 127.30, 126.48, 123.12, 120.87, 120.26, 119.88, 109.95, 77.54, 77.22, 76.90, 55.51, 40.14, 31.48, 29.60, 23.72, 22.57, 14.03.

Synthesis of 2-(9,9-dihexyl-9H-fluoren-2-yl)-1H-tetrazole (4)

A mixture of compound **3** (5.225 g, 14.47 mmol), $NEt_3 \cdot HCl$ (3.975 g, 28.95 mmol), NaN_3 (1.882 g, 28.95 mmol) was dissolved in dry and degassed DMF 25 mL, and stirred for 72 h at 125 ^{o}C under a nitrogen atmosphere. After cooling to room temperature, the solution was poured into water and extracted with ethyl acetate. The organic phase was dried over anhydrous sodium sulfate, filtered, and

concentrated to dryness. The crude was purified by column chromatography on silica gel to afford a white powder **4** (15.6 g, 9.84 mmol, 68%). ^{1}H NMR (400 MHz, $CDCl_3$) δ = 8.44 (d, *J*=0.9, 1H), 8.36 (dd, *J*=8.0, 1.4, 1H), 7.90 (d, *J*=7.9, 1H), 7.77 – 7.71 (m, 1H), 7.38 – 7.30 (m, 3H), 2.06 (dtd, *J*=16.6, 13.3, 6.1, 4H), 1.06 – 0.87 (m, 12H), 0.67 (t, *J*=7.1, 6H), 0.63 – 0.49 (m, 4H). ^{13}C NMR (101 MHz, $CDCl_3$) δ 152.30 (s), 151.45, 145.11, 139.76, 128.40, 127.07, 126.75, 123.03, 122.27, 121.35, 120.62, 55.69, 40.30, 31.49, 29.65, 23.80, 13.95.

Synthesis of 2-(9,9-hexyl-9H-fluoren-2-yl)-5-mesityl-1,3,4-oxadiazole (fom)

A mixture of compound **4 (**2.5 g, 6.2 mmol), 2,4,6-trimethylbenzoyl chloride (3.3 g, 18.6 mmol) was dissolved in dry and degassed pyridine 15 mL, and stirred for 24 h at 110 ^{o}C. After cooling to room temperature, hydrochloric acid was added to solution to reaction with pyridine. After stirring for 1 h, the solution was poured into water and extracted with dichloromethane. The organic phase was dried over anhydrous sodium sulfate, filtered, and concentrated to dryness. The crude was purified by column chromatography on silica gel to afford an oily liquid **fom** (2.6 g, 5.0 mmol, 80%). ^{1}H NMR (400 MHz, $CDCl_3$) δ = 8.19 (s, 1H), 8.07 (dd, *J*=7.9, 1.2, 1H), 7.83 (d, *J*=7.9, 1H), 7.78 – 7.75 (m, 1H), 7.41 – 7.34 (m, 3H), 7.01 (s, 2H), 2.37 (d, *J*=5.8, 9H), 2.06 (dd, *J*=16.2, 8.3, 4H), 1.16 – 0.98 (m, 12H), 0.76 (t, *J*=7.0, 6H), 0.65 (d, *J*=6.1, 4H). ^{13}C NMR (101 MHz, $CDCl_3$) δ 165.60, 163.74, 151.58, 144.86, 141.04, 139.86, 138.80, 128.93, 128.36, 127.11, 125.93, 123.06, 122.32, 121.32, 120.37, 55.46, 40.33, 31.53, 29.68, 23.79, 22.61, 21.35, 20.57, 14.04.

Synthesis of 2-(2,6-difluorophenyl)-5-(9,9-dihexyl-9H-fluoren-2-yl)-1,3,4-oxadiazole (fof)

A mixture of compound **4** (2.5 g, 6.2 mmol), 2,6-difluorophenyl chloride (3.28 g, 18.6 mmol) was dissolved in dry and degassed pyridine 15 mL, and stirred for 24 h at 110 ^{o}C. After cooling to room temperature, hydrochloric acid was added to solution to reaction with pyridine. After stirring for 1 h, the solution was poured into water and extracted with dichloromethane. The organic phase was dried over anhydrous sodium sulfate, filtered, and concentrated to dryness. The crude was purified by column chromatography on silica gel to afford an oily liquid **fof** (2.5 g, 5 mmol, 80%). ^{1}H

NMR (400 MHz, $CDCl_3$) δ = 8.16 (d, *J*=1.1, 1H), 8.11 (dd, *J*=7.9, 1.5, 1H), 7.84 (d, *J*=7.9, 1H), 7.80 – 7.73 (m, 1H), 7.54 (tt, *J*=8.5, 6.1, 1H), 7.42 – 7.32 (m, 3H), 7.18 – 7.07 (m, 2H), 2.14 – 1.92 (m, 4H), 1.14 – 0.95 (m, 12H), 0.74 (t, *J*=7.1, 6H), 0.62 (dt, *J*=14.1, 7.2, 4H). ^{13}C NMR (101 MHz, $CDCl_3$) δ 166.07, 151.58, 145.14, 139.81, 133.39, 128.39, 127.07, 126.28, 123.05, 121.79, 121.54, 120.51, 120.24, 112.56, 112.31, 55.48, 40.30, 31.50, 29.63, 23.75, 22.56, 13.99.

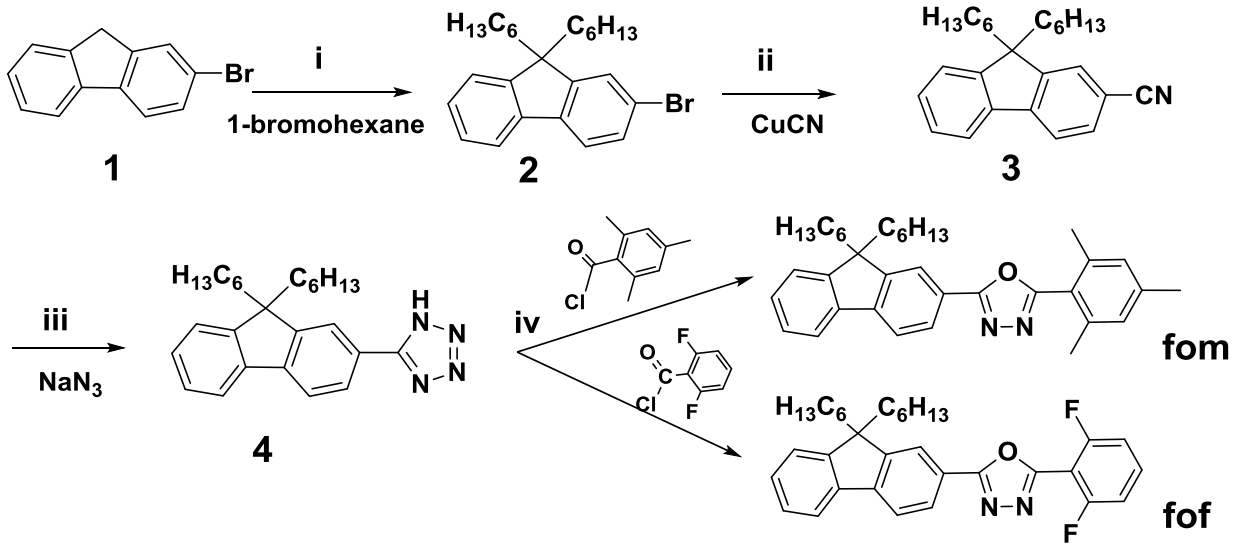

Scheme S1 Synthetic route of cyclometalating ligands **fom** and **fof**; reaction condition: (i) DMSO, 50% NaOH, TBAB, 12 h; (ii) DMF, N_2, 155 ^oC, 24 h; (iii) $NEt_3 \cdot HCl$, DMF, N_2, 125 ^oC, 72 h; (iv) pyridine, 110 ^oC, 24 h.

Synthesis of Ir(fom-Et)$_2$(pic)

The steps of the synthesis refer to complex **Ir(fom)$_2$(pic)**. ^1H NMR (400 MHz, $CDCl_3$) ^1H NMR (400 MHz, $CDCl_3$) δ = 8.29 (d, *J*=7.7, 1H), 7.93 (d, *J*=4.8, 1H), 7.83 (ddt, *J*=25.3, 16.6, 6.6, 3H), 7.59 – 7.42 (m, 5H), 7.29 (s, 2H), 7.24 (d, *J*=1.0, 4H), 7.04 (s, 4H), 2.45 (d, *J*=18.3, 12H), 2.38 (d, *J*=4.9, 6H), 1.27 (d, *J*=11.6, 10H), 0.36 (dt, *J*=26.5, 7.1, 10H). ^{13}C NMR (101 MHz, $CDCl_3$) δ = 177.41, 176.58, 173.55, 162.71, 153.02, 151.31, 151.28, 149.55, 146.18, 145.54, 145.02, 144.22, 143.70, 141.70, 141.68, 140.95, 140.50, 139.13, 138.98, 137.42, 129.13, 129.06, 128.94, 128.07, 127.61, 127.41, 127.28, 126.64, 126.48, 125.63, 125.07, 124.67, 123.06, 122.86,

120.45, 120.38, 120.30, 120.20, 119.78, 119.45, 55.50, 55.40, 32.76, 32.59, 32.46, 29.70, 21.41, 21.37, 20.96, 20.78, 8.74, 8.57.

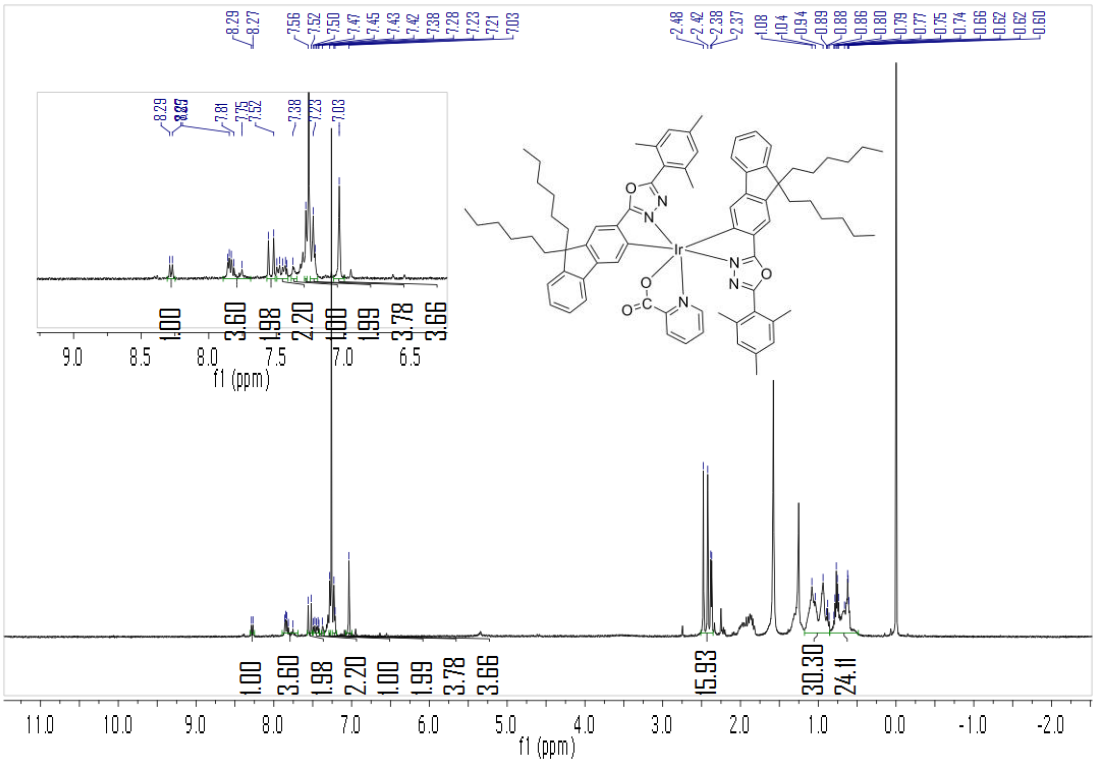

Figure S1 ^{1}H NMR spectrum of the complex **Ir(fom)$_2$(pic)**.

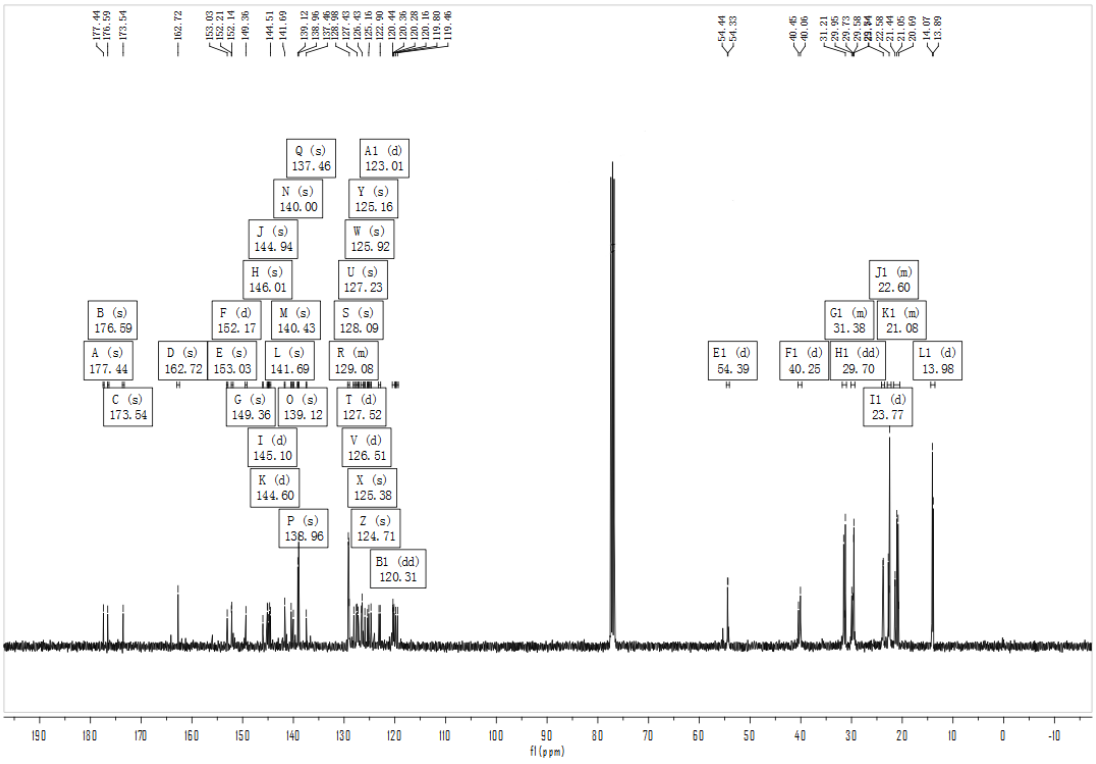

Figure S2 ^{13}C NMR spectrum of the complex **Ir(fom)$_2$(pic)**.

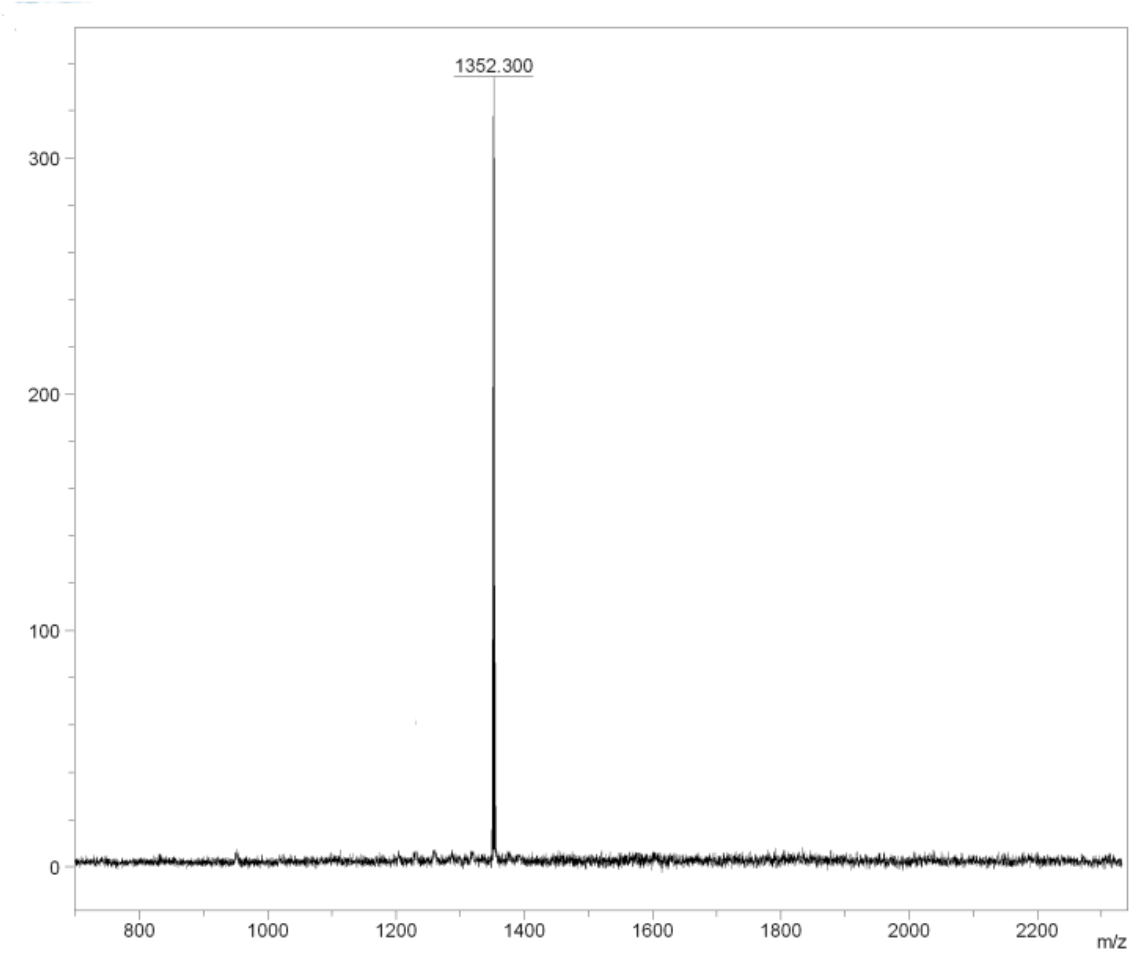

Figure S3 The MALDI-TOF mass spectrum of the complex **Ir(fom)$_2$(pic)**.

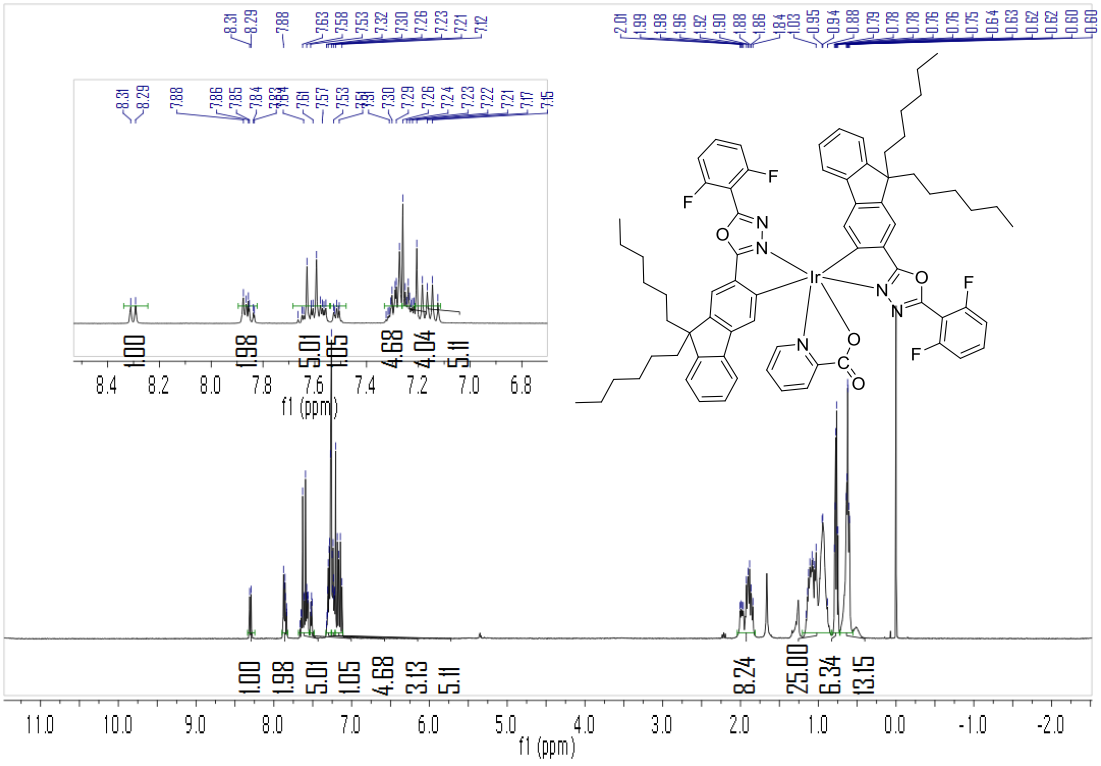

Figure S4 ^{1}H NMR spectrum of the complex **Ir(fof)$_2$(pic)**.

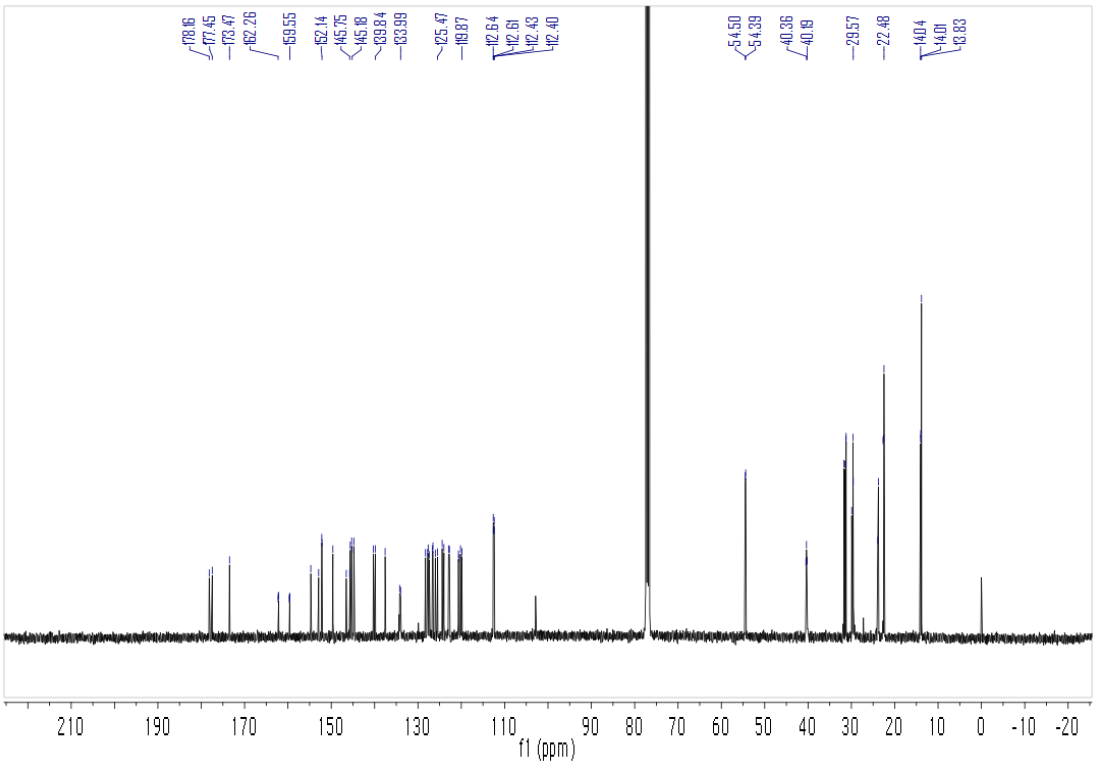

Figure S5 ^{13}C NMR spectrum of the complex **Ir(fof)$_2$(pic)**.

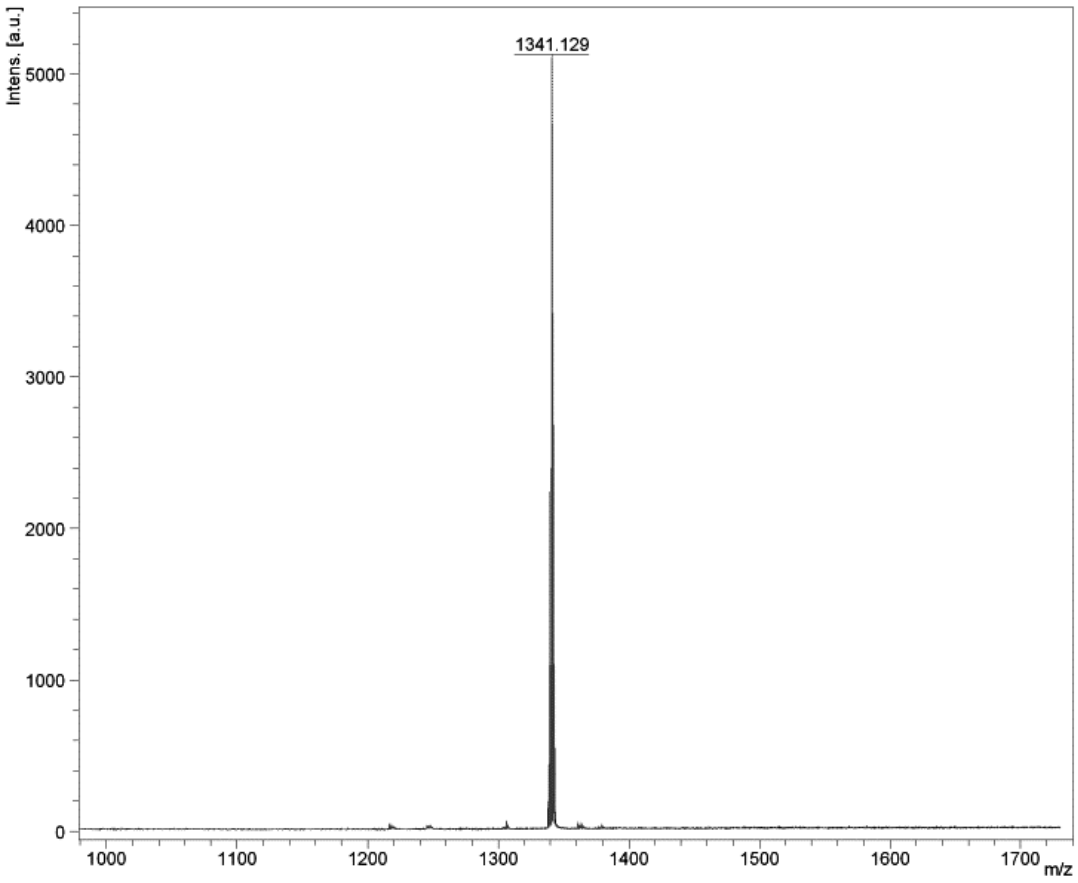

Figure S6 The MALDI-TOF mass spectrum of the complex **Ir(fof)$_2$(pic)**.

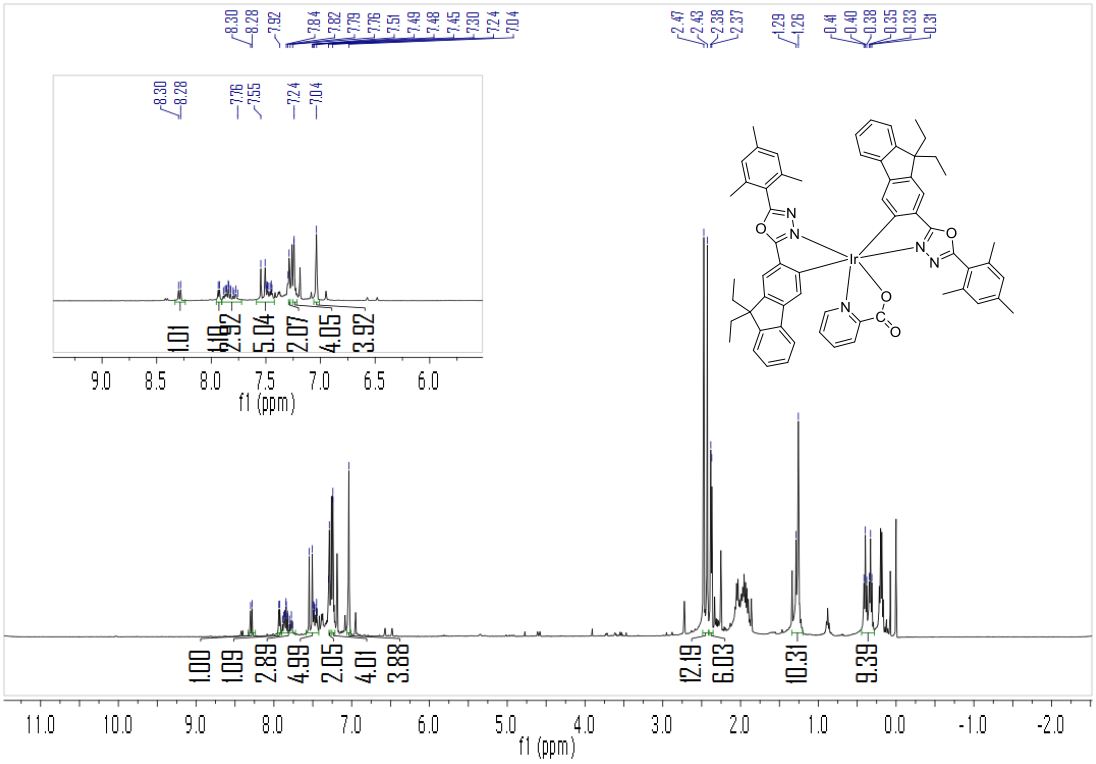

Figure S7 ^{1}H NMR spectrum of the complex **Ir(fom-Et)$_2$(pic)**.

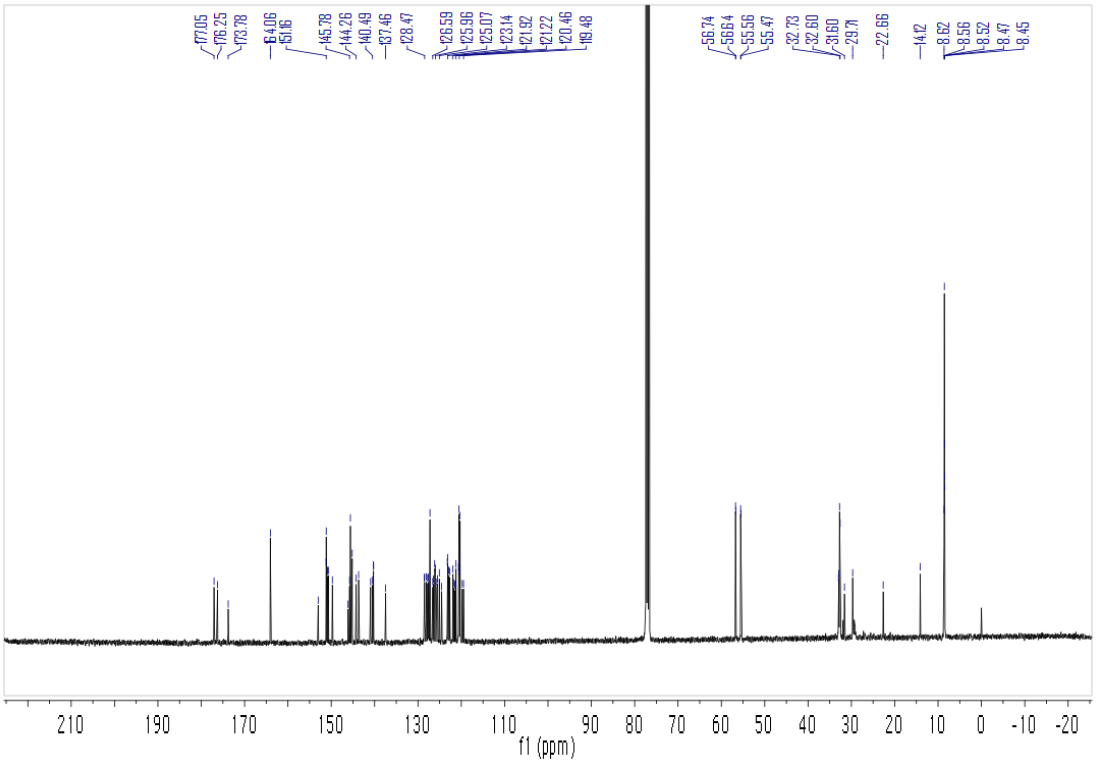

Figure S8 ^{13}C NMR spectrum of the complex **Ir(fom-Et)$_2$(pic)**.

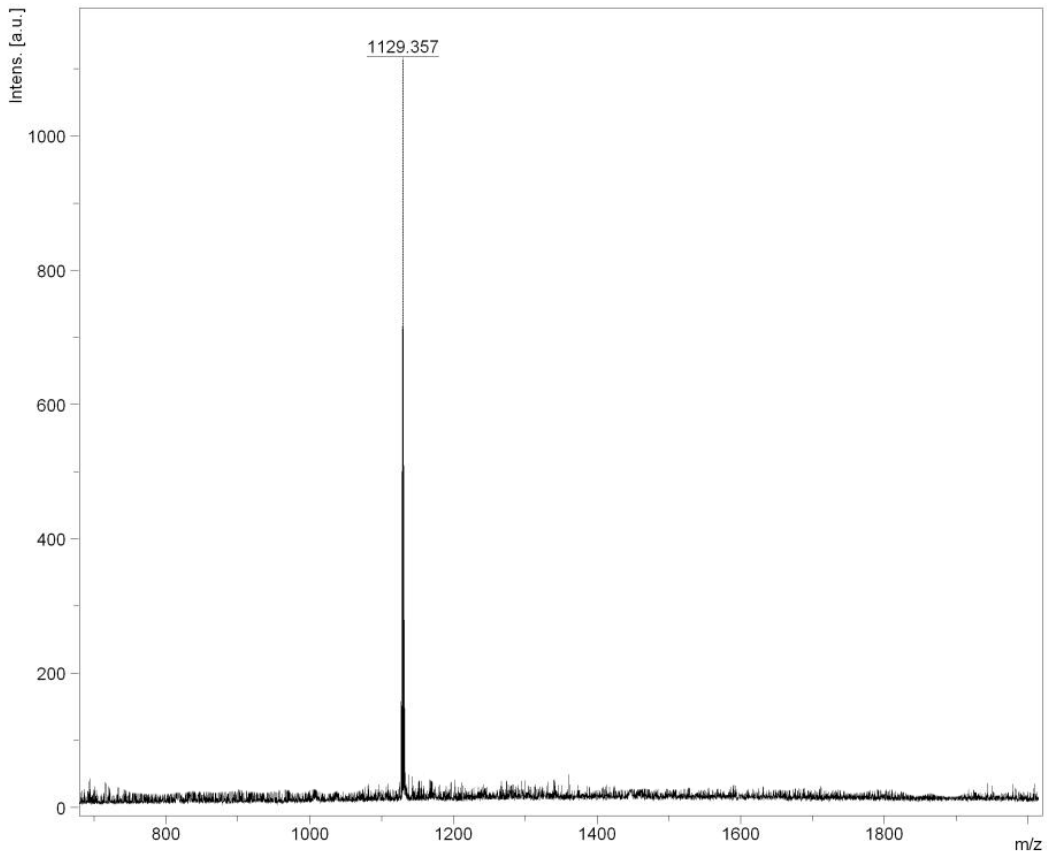

Figure S9 The MALDI-TOF mass spectrum of the complex **Ir(fom-Et)$_2$(pic)**.

Table S1 Crystallographic data of **Ir(fom-Et)$_2$(pic)**

Complex	**Ir(fom-Et)$_2$(pic)**
Formula	$C_{62}H_{58}IrN_5O_4$
Formula weight	1129.33
T(K)	100.05
Crystal system	triclinic
Space group	P-1
a/Å	15.139(6)
b/Å	15.844(6)
c/Å	16.702(7)
α/ °	64.615(7)
β/ °	76.626(9)
γ/ °	61.703(8)
V/Å^3	3185(2)

Z	2
D_{calc}g/cm^3	1.178
μ/mm^{-1}	2.140
F(000)	1148.0
Range of transm factors (deg)	2.7 to 50.018
Reflections collected	10928
Unique reflections	8053
Date/restraints/parameters	10928/448/717
Unique(R_{int})	10928(0.0563)
R_1[a],wR_2[b] [I>=2σ (I)]	0.0822, 0.1929
R_1[a],wR_2[b] [all data]	0.1151, 0.2098
GOF on F^2	1.060

R_1[a]=$\sum||F_0|-|F_c||/\sum|F_0|$, wR_2[b]=$[\sum w(F_0^2 - F_c^2)/\sum w(F_0^2)]^{1/2}$.
GOF=$[(\sum w|F_0| - |F_c|)^2/(N_{obs} - N_{param})]^{1/2}$.

Table S2 Selected bond lengths (Å) and selected bond angles (°) of **Ir(fom-Et)$_2$(pic)**

Bond length	Parameter (Å)
Ir1-N3	2.047(7)
Ir1-N2	2.038(7)
Ir1-C17	2.044(9)
Ir1-C45	2.032(9)
Ir1-O3	2.209(10)
Ir1-N5	2.079(16)

Angle	Parameter (°)
N3-Ir1-O3	100.7(3)
N3-Ir1-N5	99.1(6)
N2-Ir1-N3	171.5(3)
N2-Ir1-C17	93.9(3)
N2-Ir1-O3	86.4(3)
N2-Ir1-N5	88.9(6)
C17-Ir1-N3	79.4(3)

C17-Ir1-O3	176.7(4)
C17-Ir1-N5	162.7(7)
C45-Ir1-N3	95.2(4)
C45-Ir1-N2	80.0(3)
C45-Ir1-C17	94.2(4)
C45-Ir1-O3	89.1(4)
C45-Ir1-N5	103.1(7)
N5A-Ir1-O3	78.0(4)

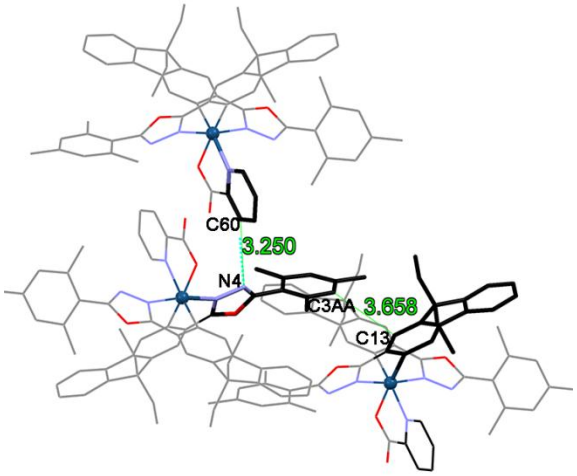

Figure S10 Partial crystal packing diagram for the case of 57.47 °dihedral angle.

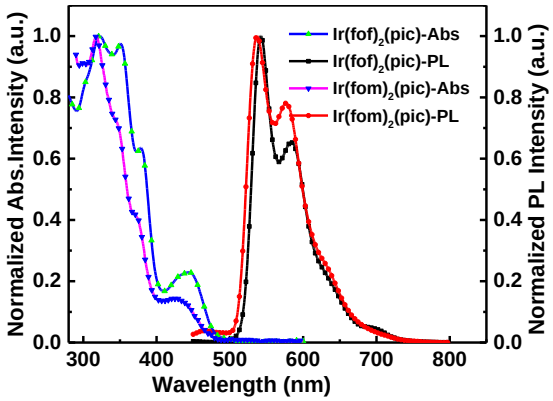

Figure S11 Absorption spectra and photoluminescence spectra of **Ir(fom)$_2$(pic)** and **Ir(fof)$_2$(pic)**.

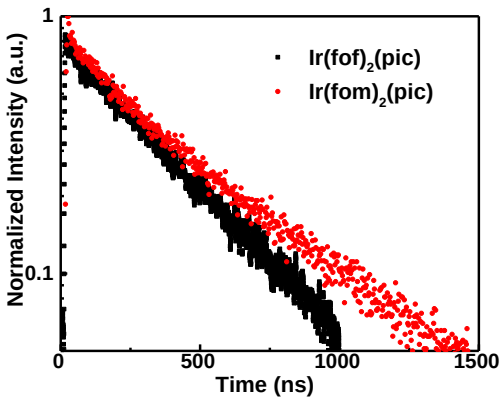

Figure S12 Excited-state lifetimes of **Ir(fom)$_2$(pic)** and **Ir(fof)$_2$(pic)**.

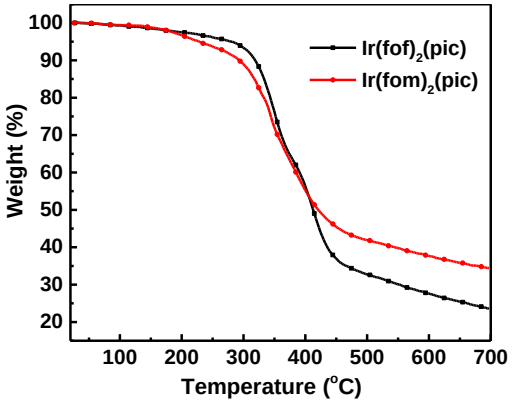

Figure S13 TGA curves of **Ir(fom)$_2$(pic)** and **Ir(fof)$_2$(pic)**.

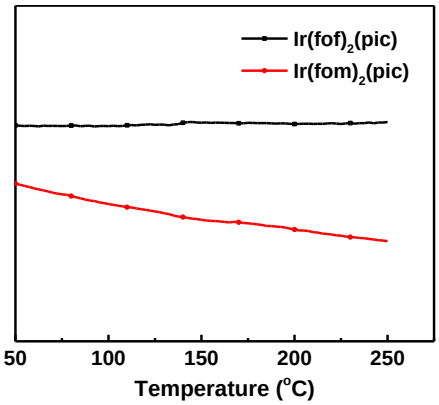

Figure S14 DSC curves of **Ir(fom)$_2$(pic)** and **Ir(fof)$_2$(pic)**.

Table S3 Absorption and photoluminescence date of the complexes.

Complex	λ_{Abs}[a] (nm)	λ_{PL}[a] (nm)	τ_1 (ns)	τ_2 (ns)	τ[b] (ns)	Φ_f[c]	T_d[d] (°C)
Ir(fom)$_2$(pic)	318, 340, 367, 427	538, 578	187.2/14.89%	586.6/85.11%	527.1	0.24	229
Ir(fof)$_2$(pic)	322, 350, 379, 443	542, 585	380.4/100%	-	380.4	0.27	279

[a] Absorption spectra and photoluminescence spectra were measured in CH_2Cl_2 solution with the

concentration of 10^{-5} M at room temperature; [b] τ lifetimes were measured in CH_2Cl_2 solution (5×10^{-5} M), λ_{exc} = 370 nm at room temperature. [c] Solid state phosphorescence quantum efficiency was determined by calibrated integrating sphere system at 298 K. [d] Temperature with 5% weight loss measured by TGA with a heating rate of 10 ^{o}C min^{-1} under N_2.

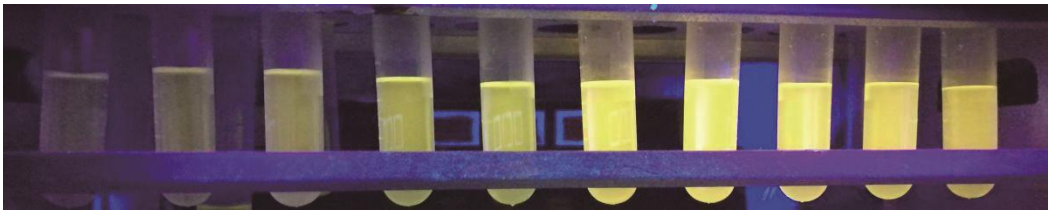

Figure S15 Photograph of **Ir(fom)$_2$(pic)** in acetone-water mixtures with different water volume fractions (f_w) taken under UV illumination (λ_{exc} = 365 nm).

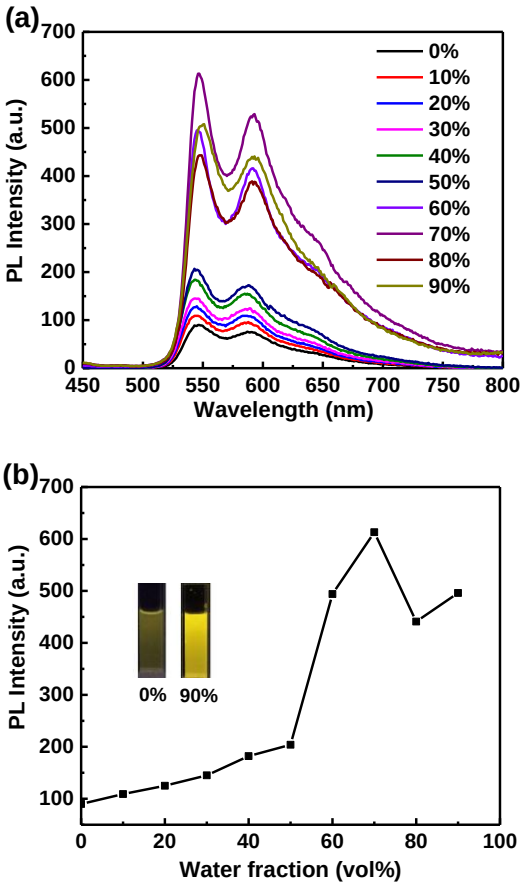

Figure S16 (a) Emission spectra of **Ir(fom-Et)$_2$(pic)** (10^{-5} M) in acetone-water mixtures with different water fractions (0-90%) at room temperature (λ_{exc} = 410 nm). (b) The profile of PL peak intensity vs. acetone-water mixtures with different water fractions (0-90%).

The electrochemical properties of complexes were examined by cyclic voltammetry in CH_2Cl_2 solution with tetrabutylammonium hexafluorophosphate

(0.10 mol L^{-1}) as supporting electrolyte. The HOMO energy level was estimated according to the following equation (1) from the onset of oxidation potential relative to the vacuum level. The LUMO energy level was calculated by the equation (2). E_g was estimated by the low energy cutoff wavelength of the absorption spectrum. All the results are summarized in Table S4.

$$E_{HOMO} = -[E_{ox} - E_{(fc/fc+)} + 4.8]\ eV \quad (1)$$

$$E_{LUMO} = E_{HOMO} + E_g,\ E_g = 1240/\lambda_{cutoff} \quad (2)$$

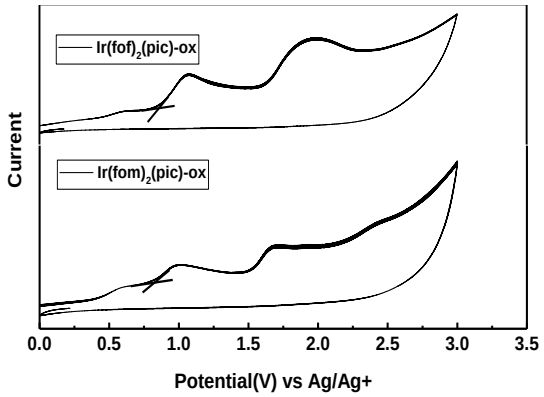

Figure S17 Cyclic voltammetry curves of **Ir(fom)$_2$(pic)** and **Ir(fof)$_2$(pic)**.

Table S4 Electrochemical for **Ir(fom)$_2$(pic)** and **Ir(fof)$_2$(pic)**

complex	E_{ox}^{cv} (V)	HOMO ^{cv} (eV)	LUMO ^{cv} (eV)	$E_g^{opt\ [a]}$ (eV)
Ir(fom)$_2$(pic)	0.83	-5.49	-2.97	2.52
Ir(fof)$_2$(pic)	0.87	-5.53	-3.13	2.40

[a] optical band gap, estimated from the absorption edge.

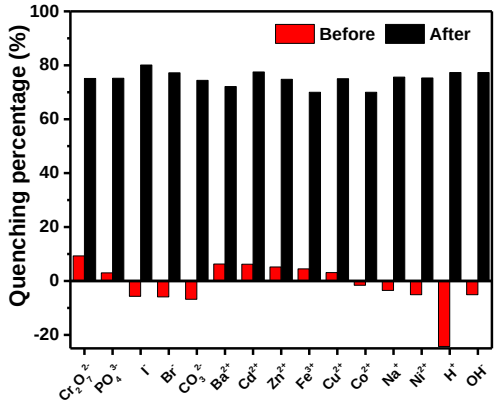

Figure S18 Quenching percentage of complex **Ir(fom)$_2$(pic)** obtained for addition of different potassium salt (including $Cr_2O_7^{2-}$, PO_4^{3-}, I^-, Br^-, CO_3^{2-}) and chloride salt (including Ba^{2+}, Cd^{2+}, Zn^{2+}, Fe^{3+}, Cu^+, Co^{2+}, Na^+, Ni^{2+}) (20 μL, 10^{-2} M), pH condition (pH = 1, pH = 14), and after addition of PA (20 μL, 10^{-2} M).

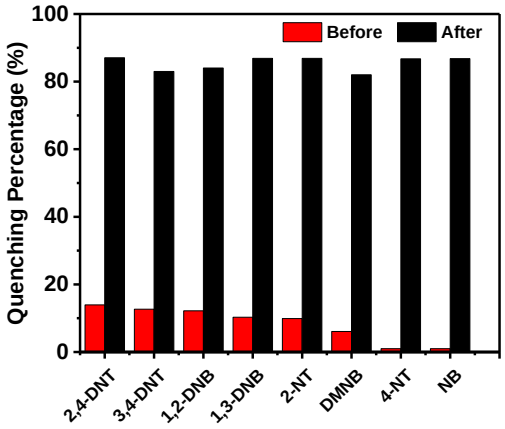

Figure S19 Quenching percentage of complex **Ir(fom)$_2$(pic)** with analytes (20 μL) in acetone–water (V/V = 3:7) mixtures before and after addition of 20 μL PA.

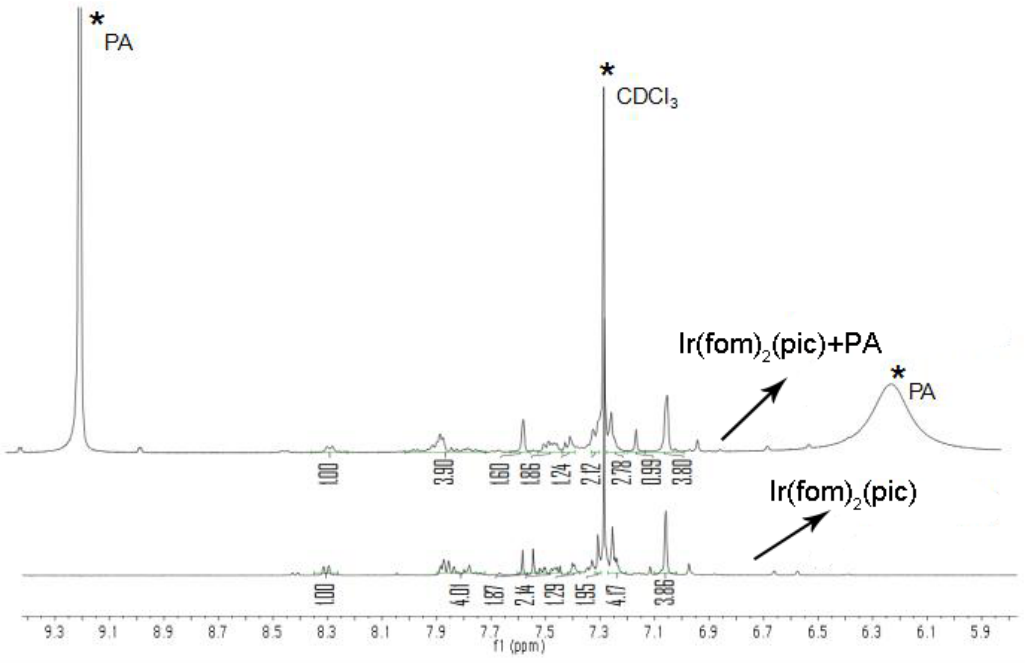

Figure S20 ^{1}H NMR spectra of complex **Ir(fom)$_2$(pic)** before and after addition of PA.

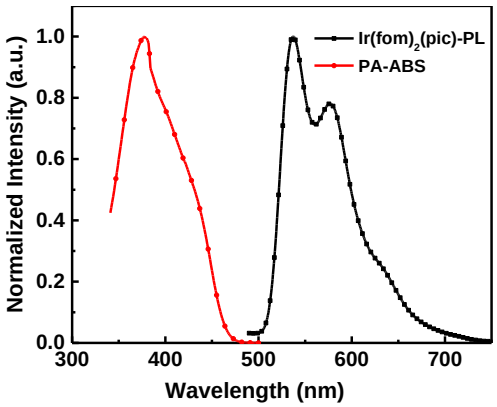

Figure S21 Absorption spectrum of PA and emission spectrum of **Ir(fom)$_2$(pic)**.

Table S5 Comparison with previous reports.

Number	Quenching constants K_{sv} (M^{-1})	Limit of detection (M)	Ref.
1	3.37×10^4	3.17×10^{-7}	This work
2	4.60×10^4	9.80×10^{-7}	1
3	4.05×10^4	1.87×10^{-7}	2
4	3.79×10^6	1.00×10^{-8}	3
5	8.00×10^4	1.00×10^{-7}	4
6	1.90×10^5	6.5×10^{-8}	5
7	3.2×10^5	1.5×10^{-7}	6
8	3.50×10^4	NA	7
9	2.9×10^4	NA	8

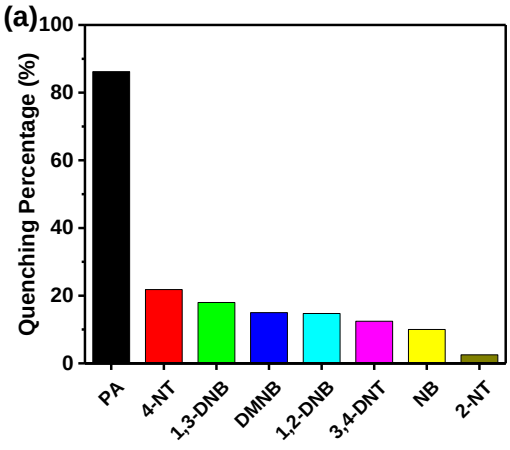

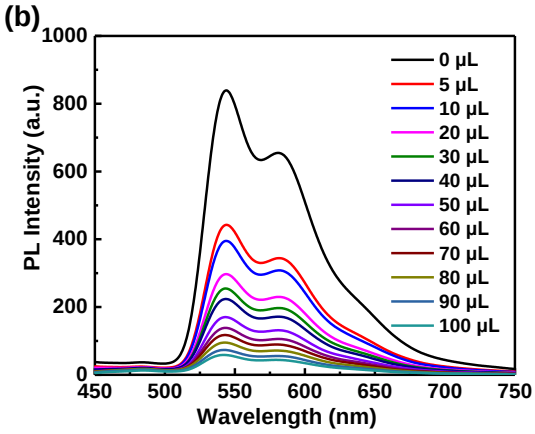

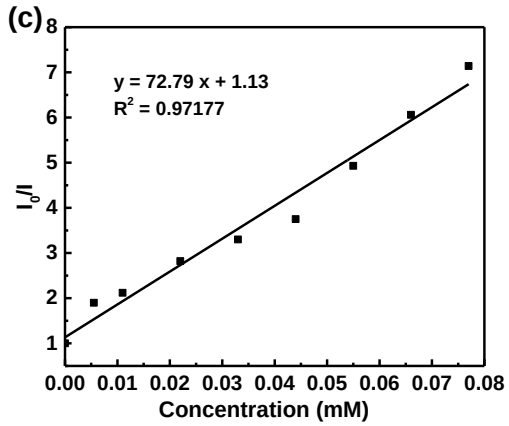

Figure S22 **(a)** Quenching percentage of complex **Ir(fom)$_2$(pic)** obtained for different analytes (20 µL) in acetone–water (V/V = 1:9) mixture; (b) PL spectra of complex **Ir(fom)$_2$(pic)** in acetone–water (V/V = 1:9) containing different amounts of PA; (c) Corresponding Stern–Volmer plot.

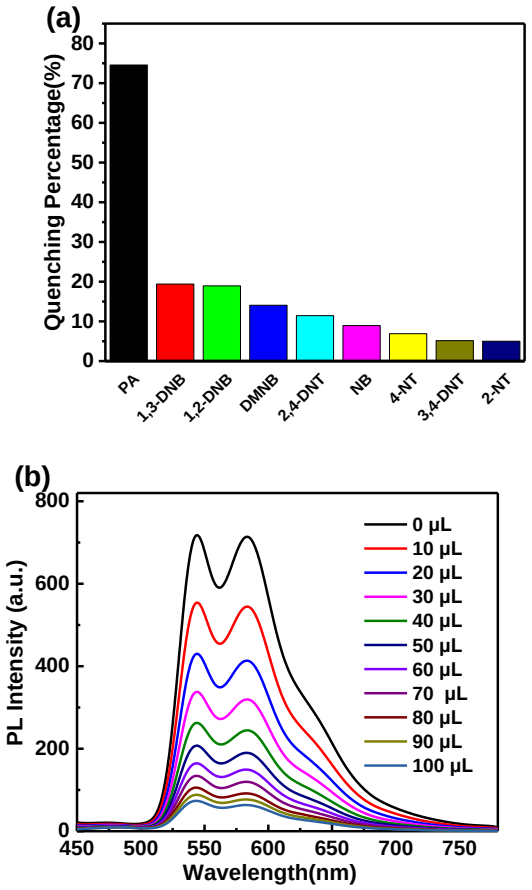

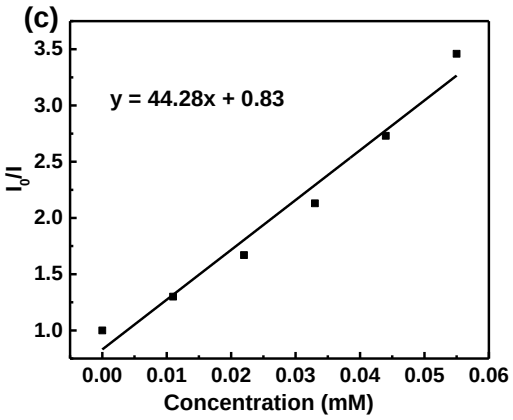

Figure S23 (a) Quenching percentage of complex **Ir(fof)$_2$(pic)** obtained for different analytes (20 μL, 10^{-2} M); (b) PL spectra of complex **Ir(fof)$_2$(pic)** in acetone–water (V/V = 1:9) containing different amounts of PA; (c) Corresponding Stern–Volmer plot of PA.

References

1. R. Lv, J. Wang, Y. Zhang, H. Li, L. Yang, S. Liao, W. Gu and X. Liu, *J. Mater. Chem. A* 2016, **4**, 15494-15500.
2. A. Buragohain, M. Yousufuddin, M. Sarma and S. Biswas, *Cryst. Growth. Des.* 2016, **16**, 842-851.
3. L.-L. Wen, X.-G. Hou, G.-G. Shan, W.-L. Song, S.-R. Zhang, H.-Z. Sun and Z.-M. Su, *J. Mater. Chem. C* 2017, **5**, 10847-10854.
4. Z. Li, Y. Q. Dong, J. W. Y. Lam, J. Sun, A. Qin, M. Haeussler, Y. P. Dong, H. H. Y. Sung, I. D. Williams, H. S. Kwok and B. Z. Tang, *Adv. Funct. Mater.* 2009, **19**, 905-917.
5. P. Alam, G. Kaur, V. Kachwal, A. Gupta, A. R. Choudhury and I. R. Laskar, *J. Mater. Chem. C* 2015, **3**, 5450-5456.
6. W. Che, G. Li, X. Liu, K. Shao, D. Zhu, Z. Su and M. R. Bryce, *Chem Commun (Camb)*, 2018, **54**, 1730-1733.
7. J. H. Lee, J. Jaworski and J. H. Jung, *Nanoscale*, 2013, **5**, 8533-8540.
8. S. S. Nagarkar, A. V. Desai and S. K. Ghosh, *Chem Commun (Camb)*, 2014, **50**, 8915-8918.